

**437**

**ASTÉRISQUE**

**2022**

COLORED STOCHASTIC VERTEX MODELS  
AND THEIR SPECTRAL THEORY

Alexei BORODIN & Michael WHEELER

**SOCIÉTÉ MATHÉMATIQUE DE FRANCE**

---

Astérisque est un périodique de la Société Mathématique de France.

Numéro 437, 2022

---

**Comité de rédaction**

Marie-Claude ARNAUD      Alexandru OANCEA  
Christophe BREUIL      Nicolas RESSAYRE  
Philippe EYSSIDIEUX      Rémi RHODES  
Colin GUILLARMOU      Sylvia SERFATY  
Fanny KASSEL      Sug Woo SHIN  
Eric MOULINES  
Nicolas BURQ (dir.)

**Diffusion**

Maison de la SMF      AMS  
Case 916 - Luminy      P.O. Box 6248  
13288 Marseille Cedex 9      Providence RI 02940  
France      USA  
commandes@smf.emath.fr      <http://www.ams.org>

**Tarifs**

Vente au numéro : 49 € (\$74)  
Abonnement Europe : 665 €, hors Europe : 718 € (\$1077)  
Des conditions spéciales sont accordées aux membres de la SMF.

**Secrétariat**

Astérisque  
Société Mathématique de France  
Institut Henri Poincaré, 11, rue Pierre et Marie Curie  
75231 Paris Cedex 05, France  
Fax: (33) 01 40 46 90 96  
asterisque@smf.emath.fr • <http://smf.emath.fr/>

© Société Mathématique de France 2022

Tous droits réservés (article L 122-4 du Code de la propriété intellectuelle). Toute représentation ou reproduction intégrale ou partielle faite sans le consentement de l'éditeur est illicite. Cette représentation ou reproduction par quelque procédé que ce soit constituerait une contrefaçon sanctionnée par les articles L 335-2 et suivants du CPI.

ISSN: 0303-1179 (print) 2492-5926 (electronic)

ISBN 978-2-85629-963-0

doi:10.24033/ast.1180

Directeur de la publication : Fabien Durand

---

**437**

**ASTÉRISQUE**

**2022**

**COLORED STOCHASTIC VERTEX MODELS  
AND THEIR SPECTRAL THEORY**

Alexei BORODIN & Michael WHEELER

**SOCIÉTÉ MATHÉMATIQUE DE FRANCE**

*Alexei Borodin*

Department of Mathematics, MIT, Cambridge, USA, and Institute for Information  
Transmission Problems, Moscow, Russia.

`borodin@math.mit.edu`

*Michael Wheeler*

School of Mathematics and Statistics, The University of Melbourne, Parkville, Victo-  
ria, Australia.

`wheelerm@unimelb.edu.au`

Texte soumis le 11 septembre 2018, révisé le 28 novembre 2020, accepté le 25 avril 2022.

---

**Mathematical Subject Classification (2010).** — 05E05, 05E10; 60J27, 82B23.

**Keywords.** — Integrable models, vertex models, orthogonal polynomials, stochastic processes.

**Mots-clés.** — Modèles intégrables, modèles de sommets, polynômes orthogonaux, processus stochas-  
tiques.

# COLORED STOCHASTIC VERTEX MODELS AND THEIR SPECTRAL THEORY

by Alexei BORODIN & Michael WHEELER

**Abstract.** — This work is dedicated to  $\mathfrak{sl}_{n+1}$ -related integrable stochastic vertex models; we call such models *colored*. We prove several results about these models, which include the following:

1. We construct the basis of (rational) eigenfunctions of the colored transfer-matrices as partition functions of our lattice models with certain boundary conditions. Similarly, we construct a dual basis and prove the corresponding orthogonality relations and Plancherel formulae.
2. We derive a variety of combinatorial properties of those eigenfunctions, such as branching rules, exchange relations under Hecke divided-difference operators, (skew) Cauchy identities of different types, and monomial expansions.
3. We show that our eigenfunctions are certain (non-obvious) reductions of the nested Bethe Ansatz eigenfunctions.
4. For models in a quadrant with domain-wall (or half-Bernoulli) boundary conditions, we prove a matching relation that identifies the distribution of the colored height function at a point with the distribution of the height function along a line in an associated color-blind ( $\mathfrak{sl}_2$ -related) stochastic vertex model. Thanks to a variety of known results about asymptotics of height functions of the color-blind models, this implies a similar variety of limit theorems for the colored height function of our models.
5. We demonstrate how the colored/uncolored match degenerates to the colored (or multi-species) versions of the ASEP,  $q$ -PushTASEP, and the  $q$ -boson model.
6. We show how our eigenfunctions relate to non-symmetric Cherednik-Macdonald theory, and we make use of this connection to prove a probabilistic matching result by applying Cherednik-Dunkl operators to the corresponding non-symmetric Cauchy identity.

**Résumé.** (Modèles de sommets stochastiques colorés et leur théorie spectrale) — Cet ouvrage est dédié aux modèles de sommets stochastiques intégrables liés à l'algèbre  $\mathfrak{sl}_{n+1}$ ; nous appelons ces modèles *colorés*. Nous prouvons plusieurs résultats sur ces modèles, dont les suivants :

1. Nous construisons la base de fonctions propres (rationnelles) des matrices de transfert colorées en tant que fonctions de partition de nos modèles. De même, nous construisons une base duale et prouvons les relations d'orthogonalité et les formules de Plancherel correspondantes.
2. Nous dérivons une variété de propriétés combinatoires de ces fonctions propres, telles que les règles de branchement, les relations d'échange sous les opérateurs de différences divisées de Hecke, les identités de Cauchy de types différents et les développements de monômes.
3. Nous montrons que nos fonctions propres sont des réductions (non évidentes) des fonctions propres du «*nested Bethe Ansatz*».
4. Pour les modèles dans un quadrant avec des conditions aux limites de type «*domain wall*» (ou «*half-Bernoulli*»), nous prouvons une relation qui identifie la distribution de la fonction de hauteur colorée en un point avec la distribution de la fonction de hauteur non-colorée le long d'une ligne dans le modèle à six sommets (lié à l'algèbre  $\mathfrak{sl}_2$ ). Grâce à une variété de résultats connus sur les asymptotiques des fonctions de hauteur non-colorées, cela implique une variété similaire de théorèmes pour la fonction de hauteur colorée de nos modèles.
5. Nous démontrons comment la correspondance colorée/non-colorée dégénère en versions colorées des modèles «*ASEP*», «*q-PushTASEP*» et «*q-boson*».
6. Nous montrons comment nos fonctions propres sont liées à la théorie non symétrique de Cherednik-Macdonald, et nous utilisons cette connexion pour prouver une correspondance probabiliste en appliquant les opérateurs de Cherednik-Dunkl à l'identité de Cauchy non symétrique.

# CONTENTS

<b>1. Introduction</b> .....	1
1.1. Preface .....	1
1.2. The model .....	4
1.3. The transfer-matrix and its eigenfunctions .....	6
1.4. Plancherel theory .....	7
1.5. Summation identities, recursive relations, monomial expansions .....	9
1.6. Matching distributions .....	13
1.7. Matching for interacting particle systems .....	16
1.8. Asymptotics .....	18
1.9. A word about extensions .....	19
1.10. Acknowledgments .....	19
<b>2. Rank-<math>n</math> vertex models</b> .....	21
2.1. Stochastic $U_q(\widehat{\mathfrak{sl}}_{n+1})$ $R$ -matrix .....	21
2.2. Higher-spin $L$ and $M$ -matrices .....	24
2.3. Intertwining equations .....	28
2.4. Color-blindness results .....	30
2.5. Stochastic weights .....	34
<b>3. Row operators and non-symmetric rational functions</b> .....	37
3.1. Space of states and row operators .....	37
3.2. Commutation relations .....	38
3.3. Colored compositions .....	43
3.4. The rational non-symmetric functions $f_\mu$ and $g_\mu$ .....	45
3.5. Permuted boundary conditions .....	50
3.6. Pre-fused functions .....	50
<b>4. Branching rules and summation identities</b> .....	55
4.1. Skew functions $f_{\mu/\nu}$ and $g_{\mu/\nu}$ .....	55
4.2. Branching rules .....	57
4.3. Summation identities of Mimachi-Noumi type .....	58
4.4. Symmetric rational function $G_{\mu/\nu}$ .....	60
4.5. Cauchy identities .....	62
<b>5. Recursive properties and symmetries</b> .....	65
5.1. Factorization of $f_\delta$ .....	65
5.2. Hecke algebra and its polynomial representation .....	66
5.3. Exchange relations for $f_\mu$ .....	67

5.4. Symmetry in $(x_i, x_{i+1})$ for $\mu_i = \mu_{i+1}$ .....	76
5.5. Relationship between $f_\mu$ and $f_\delta^\sigma$ .....	77
5.6. Relationship between $f_\mu$ and $g_\mu$ .....	79
5.7. Relationship between $f_\delta^\sigma$ and $g_\mu$ .....	82
5.8. Exchange relations for $g_\mu$ .....	82
5.9. Reduction to non-symmetric Hall-Littlewood polynomials .....	83
5.10. Eigenrelation for the non-symmetric Hall-Littlewood polynomials ..	87
<b>6. Monomial expansions: permutation graphs</b> .....	<b>91</b>
6.1. Warm-up: $F$ -matrices for two-site spin chains .....	91
6.2. $N$ -site $R$ -matrices .....	93
6.3. Permutation graphs .....	94
6.4. Reversed permutation graphs .....	96
6.5. $F$ -matrices for spin chains of generic length .....	96
6.6. Column operators .....	98
6.7. Monomial expansions .....	99
<b>7. Monomial expansions: degenerations of nested Bethe vectors</b> .....	<b>107</b>
7.1. Bethe vector blocks .....	107
7.2. Bethe vector components .....	110
7.3. Symmetrization formula for the Bethe vector components .....	110
7.4. Degenerations .....	114
7.5. Symmetrization formula for $f_\mu$ .....	116
<b>8. Orthogonality</b> .....	<b>119</b>
8.1. Scalar product .....	119
8.2. Orthogonality of $f_\mu$ and $g_\nu^*$ .....	121
<b>9. Plancherel isomorphisms</b> .....	<b>129</b>
9.1. Extending to compositions with negative parts .....	129
9.2. Function spaces .....	130
9.3. Forward transform $\mathfrak{G}$ and inverse transform $\mathfrak{F}$ .....	132
9.4. Plancherel isomorphisms .....	133
9.5. An integral formula for $G_{\mu/\nu}$ .....	136
<b>10. Matching distributions</b> .....	<b>139</b>
10.1. Path distributions in the stochastic six-vertex model, $\mathbb{P}_{6v}(\mathcal{J}, \mathcal{J})$ ...	139
10.2. Colored path distributions in the quadrant, $\mathbb{P}_{\text{col}}(\mathcal{J}, \mathcal{J})$ .....	141
10.3. Colored Hall-Littlewood processes and the distribution $\mathbb{P}_{\text{cHL}}(\mathcal{J}, \mathcal{J})$	143
10.4. Equivalence of $\mathbb{P}_{6v}(\mathcal{J}, \mathcal{J})$ and $\mathbb{P}_{\text{col}}(\mathcal{J}, \mathcal{J})$ .....	145
10.5. Equivalence of $\mathbb{P}_{6v}(\mathcal{J}, \mathcal{J})$ and $\mathbb{P}_{\text{cHL}}(\mathcal{J}, \mathcal{J})$ .....	154
<b>11. Alternative proof of Theorem 10.5.1 via Cherednik-Dunkl operators</b> .....	<b>159</b>
11.1. The distribution $\mathbb{P}_{6v}(\mathcal{J})$ .....	159
11.2. The distribution $\mathbb{P}_{\text{cHL}}(\mathcal{J})$ .....	160
11.3. A simpler match of distributions .....	161
11.4. Setting up notations .....	161
11.5. Expectations from the action of $\tilde{Y}_i$ on the Cauchy kernel .....	162



11.6. Integral expression for expectations .....	163
11.7. Matching with the six-vertex model height function .....	166
11.8. Reduction to non-symmetric Hall-Littlewood measures .....	167
11.9. Matching the underlying distributions .....	168
11.10. Hall-Littlewood difference operators .....	169
11.11. Restoring the subset $\mathcal{J}$ .....	170
11.12. A match between Cherednik-Dunkl and Macdonald difference operators .....	171
<b>12. Reduction to one-dimensional systems of particles .....</b>	<b>175</b>
12.1. Higher spin vertex model with inhomogeneous spins .....	175
12.2. Higher spin partition functions $\mathbb{Z}_{M,N}(\mathcal{J}, \mathcal{J})$ and $\mathbb{X}_{M,N}(\mathcal{J}, \mathcal{J})$ .....	175
12.3. Reduction to ASEP .....	179
12.4. Reduction to $q$ -bosons .....	185
12.5. Reduction to $q$ -PushTASEP .....	190
<b>APPENDICES</b>	
<b>A. Matching with [65] .....</b>	<b>195</b>
<b>B. Fusion .....</b>	<b>197</b>
B.1. Row-vertices .....	197
B.2. $M$ -fused vertices .....	198
B.3. Stacking $M$ -fused vertices .....	201
B.4. Evaluation of $M$ -fused vertices and analytic continuation .....	203
<b>C. Three intertwining equations .....</b>	<b>207</b>
C.1. Bosnjak-Mangazeev solution of the Yang-Baxter equation .....	207
C.2. First intertwining equation, (2.3.1) .....	209
C.3. Second intertwining equation, (2.3.2) .....	210
C.4. Third intertwining equation, (2.3.3) .....	211
C.5. Gauge transformations .....	212
<b>Index .....</b>	<b>215</b>
<b>Bibliography .....</b>	<b>219</b>



# CHAPTER 1

## INTRODUCTION

### 1.1. Preface

Exactly solvable models of Statistical Mechanics is a very well developed subject with an illustrious history that spans Mathematics, Physics, and Chemistry. Its traditional goals have been analyzing thermodynamic equilibrium in various models of Statistical Mechanics, like in Onsager’s 1944 solution of the two-dimensional Ising model [79], see also Baxter’s book [13]; and providing a convenient algebraic formalism for studying integrable systems in Quantum Mechanics in and out of equilibrium, cf. Jimbo-Miwa’s book [59].

A novel direction has been added in more recent years (although the pioneering work of Gwa-Spohn [54] goes back to 1992)—applying the same solvability mechanisms to *Markovian* systems, that can also be often viewed as models of Statistical Mechanics from an out-of-equilibrium perspective. Those include certain classes of interacting particles systems, with the Asymmetric Simple Exclusion Process, or ASEP, as a ubiquitous example, and directed polymers in random media, with the celebrated Kardar-Parisi-Zhang (KPZ) stochastic partial differential equation as a representative example.

The first wave of these Markovian integrable systems started in late 1990s with the papers of Johansson [60] and Baik-Deift-Johansson [10], and the key to their solvability, or *integrability*, was in (highly non-obvious) reductions to what physicists would call *free-fermion models*—probabilistic systems, many of whose observables are expressed in terms of determinants and Pfaffians.<sup>(1)</sup>

The second wave of integrable Markovian systems started in late 2000s, and their reliance on the methods developed for integrable models of Statistical and Quantum Mechanics was much more apparent. For example, looking at the earlier papers of the second wave we see that: (a) The pioneering work of Tracy-Widom [87, 86, 88] on the ASEP was based on the famous idea of Bethe [16] of looking for eigenfunctions of

---

1. The two-dimensional Ising model mentioned above would also be called ‘free-fermion’ in the physics literature, although it is ‘less solvable’ than the models of [60, 10] and their relatives. Statistical mechanical models of similar level of free-fermion solvability are dimer models with explicitly known coupling functions.

a quantum many-body system in the form of superposition of those for noninteracting bodies (coordinate Bethe Ansatz); (b) The work of O’Connell [78] and Borodin-Corwin [21] on semi-discrete Brownian polymers utilized properties of eigenfunctions of the Macdonald-Ruijsenaars quantum integrable system—the celebrated Macdonald polynomials and their degenerations; (c) The large time asymptotics of the physics papers of Dotsenko [48] and Calabrese-Le Doussal-Rosso [35], and a later work of Borodin-Corwin-Sasamoto [26] was based on a (previously known) duality trick that shows that certain observables of infinite-dimensional models solve finite-dimensional quantum many-body systems that are, in their turn, solvable by the coordinate Bethe Ansatz.

It turned out that all the above examples, as well as many others, can be united under a single umbrella—integrable stochastic vertex models.

Such a unification was first realized by Corwin-Petrov [43] on the basis of [17] under the name of stochastic higher spin six vertex model, see [31] for a lecture style exposition. Its existence was due to the fact that all these models were governed by the same algebraic structure—the quantum affine group  $U_q(\widehat{\mathfrak{sl}}_2)$ . This was later extended to the level of the elliptic quantum group  $E_{\tau,\eta}(\mathfrak{sl}_2)$  in [19], [2], which produced *dynamic* stochastic vertex models.

The natural next step in the ladder is the quantum groups of higher rank, and stochastic vertex models corresponding to those have been introduced by Kuniba-Mangazeev-Maruyama-Okado in [70]. In a certain degeneration, these models reproduce *multi-species* exclusion processes that have been around at least since the 1990s. A dynamic extension was given by Kuniba in [69].

Of course, one does not just want to define more and more general models; one wants to analyze their behavior in various large time and space limits and put it in the framework of universality classes.

For  $\mathfrak{sl}_2$ -related models, a few powerful approaches have been developed. Free-fermionic reductions work well for the models from the first wave and a few of those from the second wave, see [28] for a survey of the former and [18], [30], [12] for the latter. Direct analysis of integral representations of the Markov kernels (a.k.a. transfer-matrices) is sometimes possible, for either the Markovian system itself, like in [87, 86, 88], or for certain *duality functionals* (usually the  $q$ -moments) that evolve in time in a similar fashion, like in [26], [22]. Both lead to exact characterization of the large time behavior in numerous examples. A Plancherel theory for Fourier-like bases of eigenfunctions of such Markov kernels has been developed in [24], [25], [32], and derivation of the  $q$ -moments from Cauchy (reproducing kernel) identities for such functions was the central topic of [32], [19]. The  $q$ -moments can also be obtained from the eigenaction of Macdonald difference operators on Macdonald symmetric polynomials [21], [20].

For the models related to  $\mathfrak{sl}_{n+1}$  with  $n \geq 2$ , the progress has been much more modest. The only asymptotic result that we are aware of is a very recent announcement in [37] of a computation of the probability of two groups of particles of different species

to completely change their order at large times (the result is also matched to an earlier prediction by Spohn [83]). Further, to our knowledge, the only algebraic advances towards possible asymptotics appeared in recent works of Kuan, where for certain models duality functionals have been constructed (see [65] and references therein) and integral representations for transfer-matrices have been derived [66]; and in a paper by Takeyama [84], which contains a combinatorial formula for eigenfunctions of the Markov kernel for a multi-species  $q$ -boson model.

The primary goal of the present work is to advance the analysis of the  $\mathfrak{sl}_{n+1}$ -related stochastic vertex models. We call such models *colored*, because they consist of paths of different colors (that correspond to different species, in more conventional terminology). We concentrate on the *rainbow sector*, where the colors of all paths are pairwise distinct—on one hand, it is simpler algebraically, and on the other hand, rainbow stochastic model collapse onto more degenerate ones by forgetting some of the color distinctions.

Here are our main results.

- We construct the basis of (rational) eigenfunctions of the colored transfer-matrices as partition functions of our lattice models with certain boundary conditions. Similarly, we construct a dual basis and prove the corresponding orthogonality relations and Plancherel formulas. This yields an explicit integral representation of the transfer-matrices that, in particular, sheds some light on the nature of the integral representations obtained in [37].
- We derive a variety of combinatorial properties of these eigenfunctions, such as branching rules, exchange relations under Hecke divided-difference operators, (skew) Cauchy identities of different types, and monomial expansions. At the particular value  $s = 0$  of the spin parameter  $s$ , the eigenfunctions turn into non-symmetric Hall-Littlewood polynomials, and, consequently, we call them the *non-symmetric spin Hall-Littlewood functions*. We also show that the non-symmetric spin Hall-Littlewood functions are certain (non-obvious) reductions of the nested Bethe Ansatz eigenfunctions, also known as the *weight functions*.
- For the colored stochastic vertex model in a quadrant with a domain-wall (or half-Bernoulli) boundary condition, we prove a matching relation that identifies the distribution of the colored height function at a point (that encodes the colors of the paths that pass through or below this point) with the distribution of the height function along a line in an associated color-blind ( $\mathfrak{sl}_2$ -related) stochastic vertex model. Thanks to a variety of known (proved or conjectural) results about asymptotics of height functions of the color-blind models, this implies a similar variety of (proved or conjectural) limit theorems for the colored height function of our models. We also demonstrate how this colored-uncolored match degenerates to the colored (or multi-species) versions of the ASEP,  $q$ -PushTASEP, and the  $q$ -boson model.
- Another matching relation that we prove identifies the one-point distribution of the colored height function with the multi-point distribution of zeros of compositions distributed according to an ascending *non-symmetric* Hall-Littlewood process. This

is the first appearance of the non-symmetric Cherednik-Macdonald theory in a probabilistic setup, and we make use of it by proving the match by applying Cherednik-Dunkl operators to the corresponding non-symmetric Cauchy identity.

Let us now describe our results in more detail.

## 1.2. The model

The vertex models that we consider in the present work assign weights to finite collections of finite paths drawn on a square grid. Each vertex for which there exists a path that enters and exits it produces a weight that depends on the configuration of all the paths that go through this vertex. The total weight for a collection of paths is the product of weights of the vertices that the paths traverse. (Thus, we tacitly assume the normalization in which the weight of an empty vertex is always equal to 1.)

Our paths are going to be *colored*, *i.e.*, each path carries a color that is a number between 1 and  $n$ , where  $n \geq 1$  is a fixed parameter. We will usually assume that each horizontal edge of the underlying square grid can carry no more than one path, while vertical edges can be occupied by multiple paths. Thus, the states of the horizontal edges can be encoded by an integer between 0 and  $n$ , with 0 denoting an edge that is not occupied by a path, while the states of the vertical edges can be encoded by  $n$ -dimensional (nonnegative-valued) vectors which specify the number of times each color  $\{1, \dots, n\}$  appears at that edge. We will also mostly restrict ourselves to the situation when for each color there is no more than one path of this color in any path collection; in this case the vectors assigned to vertical edges will be length- $n$  binary strings.

Our paths will always travel upward in the vertical direction, and in the horizontal direction a path can travel rightward or leftward, depending on the region of the grid it is in; this choice will always be explicitly specified.

Vertex weights in the regions of rightward travel are denoted as

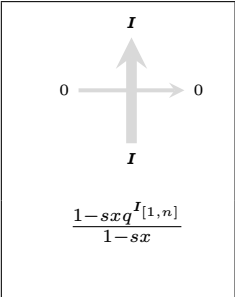
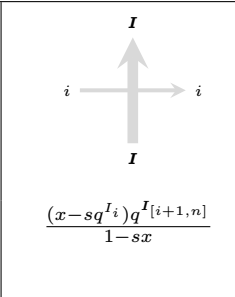
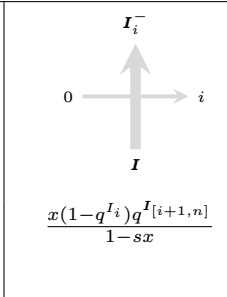
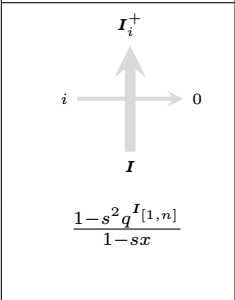
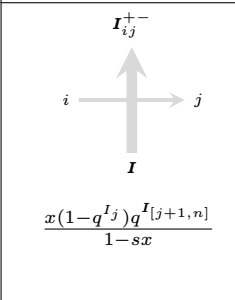
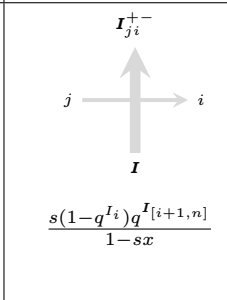
(1.2.1)

$$L_{x,q,s}(\mathbf{I}, j; \mathbf{K}, \ell) \equiv L_x(\mathbf{I}, j; \mathbf{K}, \ell) = j \begin{array}{c} \uparrow \kappa \\ \leftarrow \ell \\ \mathbf{I} \end{array}, \quad 0 \leq j, \ell \leq n, \quad \mathbf{I}, \mathbf{K} \in \{0, 1, 2, \dots\}^n,$$

where the vectors  $\mathbf{I} = (I_1, \dots, I_n)$ ,  $\mathbf{K} = (K_1, \dots, K_n)$  are chosen such that  $I_i$  (resp.,  $K_i$ ) gives the number of paths of color  $i$  present at the bottom (resp., top) edge of the vertex. The explicit values of the weights (1.2.1) are summarized in Table 1, where we assume that  $1 \leq i < j \leq n$ . Here  $q$  is the *quantization parameter*,  $s$  is the *spin parameter*, and  $x$  is the *spectral parameter*; the notation  $\mathbf{I}_{[k,n]}$  stands for  $\sum_{a=k}^n I_a$ . These weights correspond to the image of the universal  $R$ -matrix for the quantum affine group  $U_q(\widehat{\mathfrak{sl}_{n+1}})$  in the tensor product of its vector representation (horizontal

TABLE 1.

(1.2.2)

 $\frac{1 - sxq^{I[1,n]}}{1 - sx}$	 $\frac{(x - sq^{I_i})q^{I[i+1,n]}}{1 - sx}$	 $\frac{x(1 - q^{I_i})q^{I[i+1,n]}}{1 - sx}$
 $\frac{1 - s^2q^{I[1,n]}}{1 - sx}$	 $\frac{x(1 - q^{I_j})q^{I[j+1,n]}}{1 - sx}$	 $\frac{s(1 - q^{I_i})q^{I[i+1,n]}}{1 - sx}$

edges) and a Verma module (vertical edges), with the spin parameter encoding its highest weight. At  $s = q^{-\frac{N}{2}}$  with  $N \in \mathbb{Z}_{\geq 1}$ , it is easy to see that the above weights will prevent the appearance of vertical edges occupied by more than  $N$  paths; in representation theoretic language this corresponds to finite-dimensional irreducible quotients of the Verma modules that are equivalent to symmetric powers of the vector representation. In particular,  $N = 1$  forbids multiple occupation for vertical edges, and the above weights turn into a version of the  $U_q(\widehat{\mathfrak{sl}}_{n+1})$   $R$ -matrix in its defining, or fundamental, representation.

The key property of the above weights is that they satisfy the *Yang-Baxter equation*; we give a detailed account of it in Chapter 2.

A simple gauge transformation

$$(1.2.3) \quad \tilde{L}_x(\mathbf{I}, j; \mathbf{K}, \ell) := (-s)^{1_{\ell \geq 1}} \cdot L_x(\mathbf{I}, j; \mathbf{K}, \ell)$$

makes the weights (1.2.1), (1.2.2) *stochastic*, in the sense that for any fixed states of the incoming edges, the sum over all possible states of the outgoing edges is always equal to 1. Thus, if the parameters are chosen so that the modified weights are nonnegative, they can be viewed as Markovian transition probabilities. A stochastic normalization of the weights in the  $\mathfrak{sl}_{n+1}$  case first appeared in [70]; in Appendix A, we document the precise link between our notation and the one used in [65, Section 3.5].

In the regions of leftward travel, we will use a different set of weights denoted as (1.2.4)

$$M_{x,q,s}(\mathbf{I}, j; \mathbf{K}, \ell) \equiv M_x(\mathbf{I}, j; \mathbf{K}, \ell) = \ell \leftarrow \begin{array}{c} \mathbf{K} \\ \uparrow \\ \mathbf{I} \end{array} j, \quad 0 \leq j, \ell \leq n, \quad \mathbf{I}, \mathbf{K} \in \{0, 1, 2, \dots\}^n,$$

and defined by

$$(1.2.5) \quad M_{x^{-1}, q^{-1}, s^{-1}}(\mathbf{I}, j; \mathbf{K}, \ell) = (-s)^{\mathbf{1}_{\ell \geq 1} - \mathbf{1}_{j \geq 1}} \cdot L_{x,q,s}(\mathbf{I}, j; \mathbf{K}, \ell).$$

The stochastic modification takes the form  $\tilde{M}_x(\mathbf{I}, j; \mathbf{K}, \ell) := (-s)^{-\mathbf{1}_{j \geq 1}} \cdot M_x(\mathbf{I}, j; \mathbf{K}, \ell)$ .

### 1.3. The transfer-matrix and its eigenfunctions

Consider the total weight (*i.e.*, the partition function) for paths that start vertically in a prescribed configuration, end vertically in another prescribed configuration one row higher, and can move horizontally (leftward) in between. This can be illustrated pictorially as

$$(1.3.1) \quad G_{\mu/\nu}(x) = x \leftarrow \begin{array}{ccccccc} & \mathbf{B}(0) & \mathbf{B}(1) & \mathbf{B}(2) & \dots & \dots & \dots \\ & \uparrow & \uparrow & \uparrow & \uparrow & \uparrow & \uparrow \\ & \mathbf{A}(0) & \mathbf{A}(1) & \mathbf{A}(2) & \dots & \dots & \dots \end{array} 0$$

Here  $x$  is the spectral parameter used for the weights (1.2.4) in this picture,  $\mu = (\mu_1, \dots, \mu_n)$  is a *composition of length  $n$* , or a string of nonnegative integers, that gives the starting positions for paths of colors  $1, \dots, n$ , respectively,  $\nu = (\nu_1, \dots, \nu_n)$  is the composition that gives the final positions of the same paths, and the vectors  $\mathbf{A}(k), \mathbf{B}(k)$  are used to encode  $\mu$  and  $\nu$  in the grid:

$$(1.3.2) \quad \mathbf{A}(k) = \sum_{j=1}^n \mathbf{1}_{\mu_j=k} \mathbf{e}_j, \quad \mathbf{B}(k) = \sum_{j=1}^n \mathbf{1}_{\nu_j=k} \mathbf{e}_j, \quad k \in \mathbb{Z}_{\geq 0},$$

with  $\mathbf{e}_j$  denoting the  $j$ -th Euclidean unit vector.

The partition function  $G_{\mu/\nu}(x)$  is the *transfer-matrix*. As (1.2.3) and (1.2.5) show, it is simply related to the matrix of transition probabilities for a Markov chain (provided that the parameters are chosen in such a way that all entries are nonnegative).

Let us now describe our spectral representation of the transfer-matrix.

For a composition  $\mu$  and  $n$  complex parameters  $x_1, \dots, x_n$ , consider another partition function  $f_\mu(x_1, \dots, x_n)$  corresponding to the picture in Fig. 1. Here  $\mathbf{A}(k)$ 's encode  $\mu$  in the same way as in (1.3.2), and the numbers  $1, \dots, n$  next to rightward arrows on the left say that paths of colors  $1, \dots, n$  enter through the left boundary in the 1st,  $\dots$ ,  $n$ -th row, respectively (all horizontal travel is rightward). Further, the



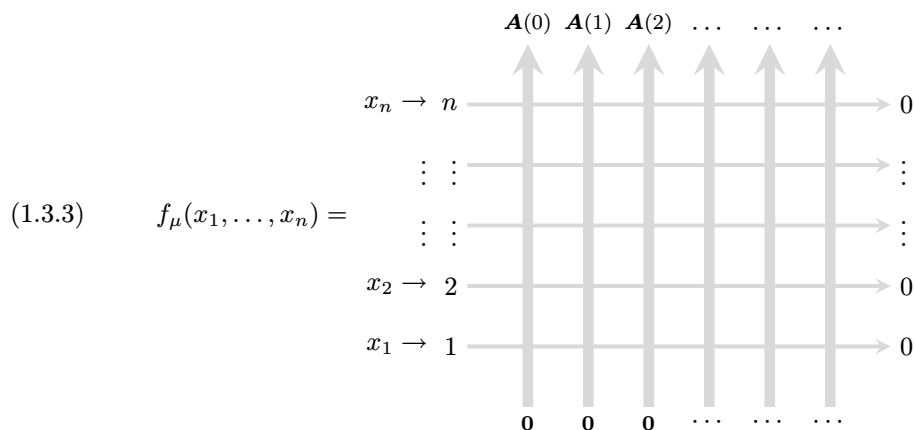


FIGURE 1.

symbols  $x_1, \dots, x_n$  say that we use those spectral parameters in the corresponding rows to compute the weights (1.2.1). The zeros on the bottom and on the right mean that no paths enter and exit there.

**Proposition 1.3.1 (Special case of Proposition 4.5.1).** — Assume  $x_1, \dots, x_n, y \in \mathbb{C}$  are such that

$$(1.3.4) \quad \left| \frac{x_i - s}{1 - sx_i} \cdot \frac{y - s}{1 - sy} \right| < 1, \quad \text{for all } 1 \leq i \leq n.$$

Then for any composition  $\nu = (\nu_1, \dots, \nu_n)$  of length  $n$  one has the identity

$$(1.3.5) \quad \sum_{\mu} f_{\mu}(x_1, \dots, x_n) G_{\mu/\nu}(y) = \prod_{i=1}^n \frac{1 - qx_i y}{q(1 - x_i y)} \cdot f_{\nu}(x_1, \dots, x_n),$$

where the summation is taken over all length- $n$  compositions  $\mu = (\mu_1, \dots, \mu_n)$ .

Equation (1.3.5) shows that  $f_{\mu}$ 's are algebraic eigenfunctions of the transfer-matrix  $G_{\mu/\nu}$ . However, since we are in infinite-dimensional space (with basis parameterized by compositions of length  $n$ ), we need some sort of spectral analysis to have any hope of using  $f_{\mu}$ 's for studying the Markov evolution. This is precisely what we explain next.

### 1.4. Plancherel theory

We need to define functional spaces on which our Fourier-like transform with kernel  $f_{\mu}(x_1, \dots, x_n)$  will act. For the clarity of exposition, we choose the smallest possible spaces; they could be extended by a natural completion procedure but we will not pursue this here.

Let  $\mathcal{C}^n$  denote the space of complex-valued, finitely supported functions on  $\mathbb{Z}^n$ , and let  $\mathcal{L}^n$  denote the space of all functions  $\Phi : \mathbb{C}^n \rightarrow \mathbb{C}$  such that (a)  $\Phi(x_1, \dots, x_n)$  is a Laurent polynomial in the variables  $(x_i - s)/(1 - sx_i)$ ,  $1 \leq i \leq n$ , and (b)  $\lim_{x_i \rightarrow \infty} \Phi(x_1, \dots, x_n) = 0$  for all  $1 \leq i \leq n$ .

We also need the dual functions  $g_\mu(x_1, \dots, x_n)$ , which can be defined as

(1.4.1)

$$g_{\tilde{\mu}}(x_n^{-1}, \dots, x_1^{-1}; q^{-1}, s^{-1}) = c_\mu(q, s) \prod_{i=1}^n x_i \cdot f_\mu(x_1, \dots, x_n; q, s), \quad \tilde{\mu} = (\mu_n, \dots, \mu_1),$$

where the multiplicative constant  $c_\mu(q, s)$  is given by

(1.4.2)

$$c_\mu(q, s) = \frac{s^n (q-1)^n q^{\text{inv}(\tilde{\mu})}}{\prod_{j \geq 0} (s^{2j}; q)_{m_j(\mu)}}, \quad \text{inv}(\tilde{\mu}) = \#\{i < j : \tilde{\mu}_i \geq \tilde{\mu}_j\} = \#\{i < j : \mu_i \leq \mu_j\},$$

with the standard  $q$ -Pochhammer definitions

$$(a; q)_m := (1-a)(1-qa) \cdots (1-q^{m-1}a), \quad m \geq 1, \quad (a; q)_0 := 1,$$

and with  $m_j(\mu) := \#\{1 \leq k \leq n : \mu_k = j\}$  for all  $j \geq 0$ ; as well as their alternative normalization

$$g_\mu^*(x_1, \dots, x_n) := q^{n(n+1)/2} (q-1)^{-n} \cdot g_\mu(x_1, \dots, x_n).$$

The functions  $g_\mu(x_1, \dots, x_n)$  can also be constructed as suitable partition functions, similarly to (1.3.3), cf. (3.4.10) below.

The functions  $f_\mu$  and  $g_\mu$  naturally extend to compositions  $\mu$  with arbitrary (not necessarily nonnegative) parts via

$$(1.4.3) \quad f_{\mu+(k, \dots, k)}(x_1, \dots, x_n) = \prod_{i=1}^n \left( \frac{x_i - s}{1 - sx_i} \right)^k f_\mu(x_1, \dots, x_n), \quad k \in \mathbb{Z},$$

and similarly for  $g_\mu$ . One checks that  $f_\mu, g_\mu \in \mathcal{L}^n$  for any  $\mu \in \mathbb{Z}^n$ .

We can now define a forward transform  $\mathfrak{G} : \mathcal{C}^n \rightarrow \mathcal{L}^n$  and an inverse transform  $\mathfrak{F} : \mathcal{C}^n \rightarrow \mathcal{L}^n$  as

$$\begin{aligned} \mathfrak{G}[\alpha](x_1, \dots, x_n) &= \sum_{\mu \in \mathbb{Z}^n} \alpha(\mu) g_\mu^*(x_1, \dots, x_n), \\ \mathfrak{F}[\Phi](\mu) &= \left( \frac{1}{2\pi\sqrt{-1}} \right)^n \oint_{C_1} \frac{dx_1}{x_1} \cdots \oint_{C_n} \frac{dx_n}{x_n} \\ &\quad \times \prod_{1 \leq i < j \leq n} \frac{x_j - x_i}{x_j - qx_i} f_\mu(\bar{x}_1, \dots, \bar{x}_n) \Phi(x_1, \dots, x_n), \end{aligned}$$

where  $\{C_1, \dots, C_n\}$  are closed, pairwise non-intersecting, positively oriented contours in the complex plane such that they all surround the point  $s$ , and the contours  $C_i$  and  $q \cdot C_i$  are both contained within contour  $C_{i+1}$  for all  $1 \leq i \leq n-1$ , where  $q \cdot C_i$  denotes the image of  $C_i$  under multiplication by  $q$ . An illustration of such contours is given in Figure 11 below (p. 120).

**Theorem 1.4.1 (Theorem 9.4.1 below).** — *The maps  $\mathfrak{F} \circ \mathfrak{G} : \mathcal{C}^n \rightarrow \mathcal{C}^n$  and  $\mathfrak{G} \circ \mathfrak{F} : \mathcal{L}^n \rightarrow \mathcal{L}^n$  both act as the identity; we have*

$$(1.4.4) \quad \mathfrak{F} \circ \mathfrak{G} = \text{id} \in \text{End}(\mathcal{C}^n), \quad \mathfrak{G} \circ \mathfrak{F} = \text{id} \in \text{End}(\mathcal{L}^n).$$

Unraveling the first of the relations (1.4.4) shows that  $\{f_\mu\}$  and  $\{g_\nu^*\}$  form biorthonormal bases in  $\mathcal{L}^n$ , cf. Theorem 8.2.1 below. For versions of Theorem 1.4.1 in the color-blind ( $\mathfrak{sl}_2$ -related) case, see [24], [25], [32] and references therein.

As a corollary of Theorem 1.4.1, one obtains a *spectral decomposition* of the transfer-matrix:

$$(1.4.5) \quad G_{\mu/\nu}(y) = \frac{q^{-n}}{(2\pi\sqrt{-1})^n} \oint_{C_1} \frac{dx_1}{x_1} \cdots \oint_{C_n} \frac{dx_n}{x_n} \\ \times \prod_{1 \leq i < j \leq n} \frac{x_j - x_i}{x_j - qx_i} \prod_{i=1}^n \frac{x_i - qy}{x_i - y} f_\nu(\bar{x}_1, \dots, \bar{x}_n) g_\mu^*(x_1, \dots, x_n).$$

For  $\mu = (\mu_1 \geq \dots \geq \mu_n)$  and  $\nu = (\nu_1 \leq \dots \leq \nu_n)$  this can be substantially simplified; see Remark 9.5.2 below, showing a certain connection with the recent work [37].

While Theorem 1.4.1 is easy to state, it was certainly not easy to prove, and understanding structural properties of the functions  $f_\mu$  is key. Let us summarize some of these properties.

### 1.5. Summation identities, recursive relations, monomial expansions

The functions  $f_\mu$ ,  $g_\mu$ , and their skew variants (defined as partition functions of the form (1.3.3), but with possibly nonempty set of paths entering through the bottom boundary), satisfy a host of summation identities that can be found in Chapter 4 below. One of those identities is (1.3.5) above. Let us reproduce another one of them here, because of its importance for (1.4.4), and also because it is strikingly similar to an identity of Mimachi-Noumi for non-symmetric Macdonald polynomials [77].

**Theorem 1.5.1.** — *(Theorem 4.3.1 below) Let  $(x_1, \dots, x_n)$  and  $(y_1, \dots, y_n)$  be two sets of complex parameters such that*

$$(1.5.1) \quad \left| \frac{x_i - s}{1 - sx_i} \cdot \frac{y_j - s}{1 - sy_j} \right| < 1, \quad \text{for all } 1 \leq i, j \leq n.$$

*Then*

$$(1.5.2) \quad \sum_{\mu} f_{\mu}(x_1, \dots, x_n) g_{\mu}^*(y_1, \dots, y_n) = \prod_{i=1}^n \frac{1}{1 - x_i y_i} \prod_{n \geq i > j \geq 1} \frac{1 - qx_i y_j}{1 - x_i y_j},$$

*where the summation is over all compositions  $\mu$  (with nonnegative coordinates).*

The similarity with non-symmetric Macdonald polynomials is not a coincidence— we prove, in Theorem 5.9.4 below, that at the value  $s = 0$  of our spin parameter, the functions  $f_\mu$  coincide with the non-symmetric Macdonald polynomials in the Hall-Littlewood specialization (Macdonald’s  $q$ -parameter vanishes, and Macdonald’s

$t$ -parameter coincides with our quantization parameter). Furthermore, color-blindness results of Section 2.4 easily show that if one sums  $f_\mu$ 's over all possible choices of colors of the top outgoing edges (equivalently, one can sum over all compositions  $\mu$  of length  $n$  whose entries, when ordered, give the same partition), one recovers the *symmetric* spin Hall-Littlewood functions introduced in [17]; this is Proposition 3.4.4 in the text.

Because of these coincidences, we call our  $f_\mu$ 's the *non-symmetric spin Hall-Littlewood functions*.

The connection to non-symmetric Macdonald theory was originally a surprise to us, largely because, to our best knowledge, the non-symmetric Macdonald polynomials (with any values of their parameters) were not known to have partition function representations<sup>(2)</sup> as in (1.3.3). We establish the connection through the following two statements.

The first one is the base for a recursion:

**Proposition 1.5.2 (Proposition 5.1.1 below).** — *Let  $\delta = (\delta_1 \leq \dots \leq \delta_n)$  be an anti-dominant composition. The corresponding non-symmetric spin Hall-Littlewood function  $f_\delta$  is completely factorized:*

$$(1.5.3) \quad f_\delta(x_1, \dots, x_n) = \frac{\prod_{j \geq 0} (s^2; q)_{m_j(\delta)}}{\prod_{i=1}^n (1 - sx_i)} \prod_{i=1}^n \left( \frac{x_i - s}{1 - sx_i} \right)^{\delta_i},$$

$$m_j(\delta) = \#\{k \in \{1, \dots, n\} : \delta_k = j\}, \quad j \geq 0.$$

The second one is the recursion itself:

**Theorem 1.5.3 (A part of Theorem 5.3.1 below).** — *Let  $\mu = (\mu_1, \dots, \mu_n)$  be a length- $n$  composition with  $\mu_i < \mu_{i+1}$  for some  $1 \leq i \leq n - 1$ . Then*

$$(1.5.4) \quad T_i \cdot f_\mu(x_1, \dots, x_n) = f_{(\mu_1, \dots, \mu_{i+1}, \mu_i, \dots, \mu_n)}(x_1, \dots, x_n),$$

where

$$(1.5.5) \quad T_i \equiv q - \frac{x_i - qx_{i+1}}{x_i - x_{i+1}}(1 - \mathfrak{s}_i), \quad 1 \leq i \leq n - 1,$$

with elementary transpositions  $\mathfrak{s}_i \cdot h(x_1, \dots, x_n) := h(x_1, \dots, x_{i+1}, x_i, \dots, x_n)$ , are the Demazure-Lusztig operators of the polynomial representation of the Hecke algebra of type  $A_{n-1}$ .

The combination of (1.5.3) and (1.5.4) provides an algorithm for evaluating  $f_\mu$ 's, but does not yield a closed formula. We offer two rather different formulas for the  $f_\mu$ 's; both represent them as sums of factorized (monomial) expressions with certain coefficients. The appearance of factorized monomials in both expansions below follows from (1.5.3).

---

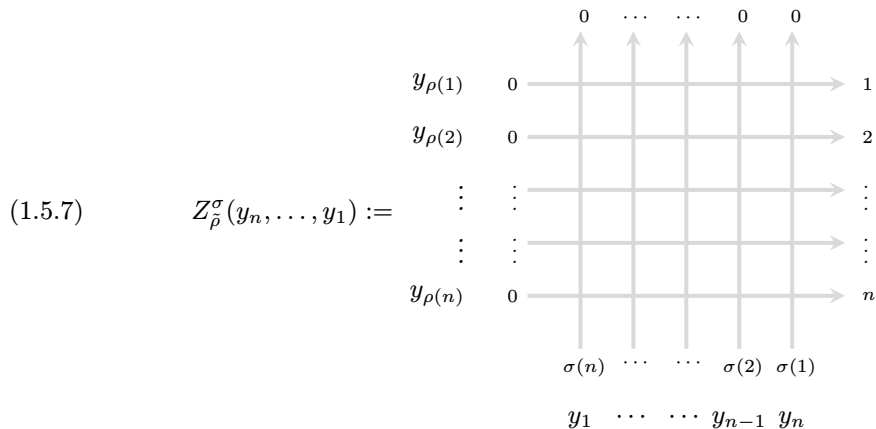
2. A partition function representation for a different family of non-symmetric polynomials, which yield symmetric Macdonald polynomials under appropriate symmetrization, was however obtained in [36].

The first monomial expression that we give plays a key role in our proof of Theorem 1.4.1.

**Theorem 1.5.4 (Combination of Theorem 5.5.1, Theorem 6.7.1, and Proposition 6.7.6 below).** — Fix a composition  $\mu$ , and let  $\delta = (\delta_1 \leq \dots \leq \delta_n)$  and  $\sigma \in \mathfrak{S}_n$  be an anti-dominant composition and a minimal-length permutation such that  $\mu_i = \delta_{\sigma(i)}$ ,  $1 \leq i \leq n$ . Then

$$(1.5.6) \quad f_\mu(x_1^{-1}, \dots, x_n^{-1}; q^{-1}, s^{-1}) = s^{-n} q^{-\text{inv}(\mu)} \prod_{i=1}^n x_i \times \sum_{\kappa \in \mathfrak{S}_n} \prod_{1 \leq a < b \leq n} \frac{x_{\kappa(b)} - qx_{\kappa(a)}}{x_{\kappa(b)} - x_{\kappa(a)}} Z_\kappa^\sigma(x_1, \dots, x_n) f_\delta(x_{\kappa(1)}, \dots, x_{\kappa(n)}; q, s),$$

where  $\text{inv}(\mu) = \#\{i < j : \mu_i \geq \mu_j\}$ , and the coefficients  $Z_\kappa^\sigma$  can be determined as follows. For any permutation  $\rho \in \mathfrak{S}_n$  with further notation  $\tilde{\rho}(i) = n - \rho(i) + 1$ ,  $Z_{\tilde{\rho}}^\sigma(y_n, \dots, y_1)$  equals the partition function in a square region of size  $n \times n$  with domain wall boundary conditions corresponding to the following picture:

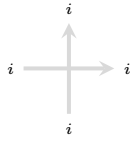
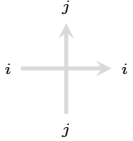
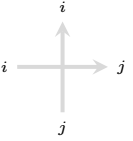
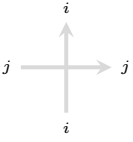
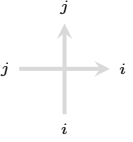


in which the  $i$ -th horizontal line (counted from the top) carries rapidity  $y_{\rho(i)}$ , left external edge state 0 and right external edge state  $i$ , while the  $j$ -th vertical line (counted from the left) carries rapidity  $y_j$ , bottom external edge state  $\sigma(n - j + 1)$  and top external edge state 0. Here no edge can be occupied by more than one path, with the vertex weights summarized in Table 2, where  $0 \leq i < j \leq n$ , and the spectral parameter  $z$  is equal to the ratio of the rapidities on the vertical and horizontal lines that cross at the corresponding vertex.

Our second monomial expansion has its origin in the nested Bethe Ansatz. We prove that the non-symmetric spin Hall-Littlewood functions are appropriate specializations of the off-shell nested Bethe vectors also known as the *weight functions*. The specializations reduce the number of free variables from  $n(n + 1)/2$  to  $n$ . Combined with a

TABLE 2.

(1.5.8)

 $1$	 $\frac{q(1-z)}{1-qz}$	 $\frac{1-q}{1-qz}$
	 $\frac{1-z}{1-qz}$	 $\frac{(1-q)z}{1-qz}$

known symmetrization formula for the nested Bethe vectors, see [85] and references therein, we obtain the following statement.

**Theorem 1.5.5 (Theorem 7.5.1 below).** — Fix a composition  $\mu = (\mu_1, \dots, \mu_n)$  and let  $\delta = (\delta_1 \leq \dots \leq \delta_n)$  be its anti-dominant reordering. Define a vector  $\gamma(\mu)$  via

$$\gamma(\mu) = (\gamma_1, \gamma_2, \dots, \gamma_n) = w_\mu \cdot (1, 2, \dots, n),$$

where  $w_\mu \in \mathfrak{S}_n$  is the minimal-length permutation such that  $w_\mu \cdot \mu = \delta$ . Further, define a sequence of vectors of decreasing lengths by

$$p^{(1)} = \gamma(\mu), \quad p^{(i+1)} = p^{(i)} \setminus \{i\}, \quad 1 \leq i \leq n - 1,$$

as well as  $n - 1$  strictly increasing integer sequences  $a^{(2)}, \dots, a^{(n)}$  that, as sets, are given by  $a^{(i)} = \{1 \leq b \leq n - i + 2 : p_b^{(i-1)} \geq i\}$ . The non-symmetric spin Hall-Littlewood functions are given by

$$\begin{aligned} f_\mu(x_n, \dots, x_1) &= \sum_{\sigma^{(1)} \in \mathfrak{S}_n} \cdots \sum_{\sigma^{(n-1)} \in \mathfrak{S}_2} f_\delta(x_{\sigma^{(1)}(1)}, \dots, x_{\sigma^{(1)}(n)}) \\ &\times \prod_{1 \leq i < j \leq n} \frac{qx_{\sigma^{(1)}(i)} - x_{\sigma^{(1)}(j)}}{x_{\sigma^{(1)}(i)} - x_{\sigma^{(1)}(j)}} \\ &\times \prod_{b=2}^n \psi_{\{a_1^{(b)}, \dots, a_{n-b+1}^{(b)}\}} \left( \sigma^{(b)} \cdot (x_1, \dots, x_{n-b+1}); \sigma^{(b-1)} \cdot (x_1, \dots, x_{n-b+2}) \right) \end{aligned}$$

$$\times \prod_{1 \leq i < j \leq n-b+1} \frac{qx_{\sigma^{(b)}(i)} - x_{\sigma^{(b)}(j)}}{x_{\sigma^{(b)}(i)} - x_{\sigma^{(b)}(j)}},$$

where by agreement  $\sigma^{(n)}$  denotes the trivial permutation  $\sigma^{(n)} = (1) \in \mathfrak{S}_1$ , and

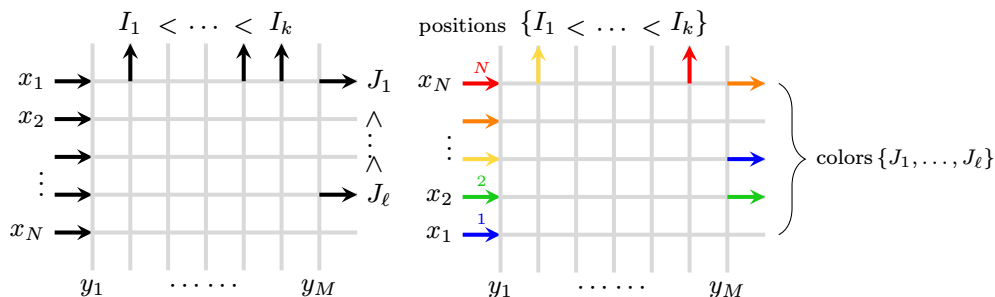
$$\psi_{\{a_1, \dots, a_m\}}(x_1, \dots, x_m; y_1, \dots, y_M) = \prod_{i=1}^m \left[ \frac{(1-q)y_{a_i}}{x_i - qy_{a_i}} \prod_{j=1}^{a_i-1} \frac{x_i - y_j}{x_i - qy_j} \right], \quad \forall 1 \leq m \leq M.$$

While Theorem 1.5.5 is not used in the rest of the work, we view it as an important bridge between what we do and the more traditional spectral approach to the higher rank vertex models in finite volume that proceeds through the nested Bethe Ansatz.

### 1.6. Matching distributions

While we fully expect the spectral representation (1.4.5) and the non-symmetric spin Hall-Littlewood functions to be effective for asymptotic analysis of colored vertex models, we do not attempt to do that in the present work. Instead, we focus on another approach that has been quite successful recently in the case of the color-blind models, cf. [18], [20], [12]. More concretely, we look for distributional matching of observables in different models. Surprisingly, we find a matching that allows one to extract probabilistic and asymptotic information for colored models from that for the color-blind ones. As the latter ones are well-studied, one can immediately carry over the known results and conjectures to the colored situation, cf. Section 1.8 below.

Our first matching statement concerns the partition functions associated with the following pictures:



The picture on the left is for the partition function in the (stochastic) color-blind model on an  $M \times N$  rectangle with no more than one path on each edge, row rapidities  $x_1, \dots, x_N$  (numbered top-to-bottom), column rapidities  $y_1, \dots, y_M$  (numbered left-to-right), and vertex weights given by (1.5.8) with  $n = 1$  and with the spectral parameter  $z$  equal to  $x_i y_j$ , where  $x_i$  and  $y_j$  are the rapidities of the vertex's row and column. The boundary conditions are specified by requiring that paths enter through every horizontal edge along the left boundary and exit through positions

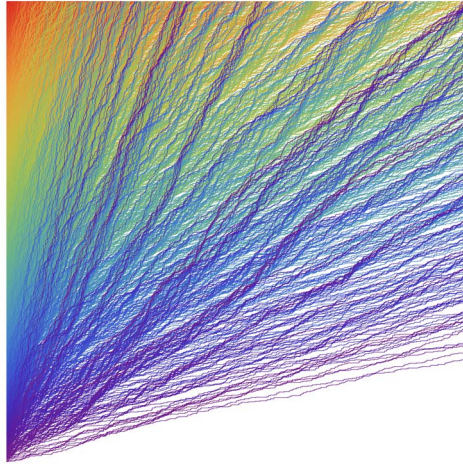


FIGURE 2. A simulation of the stochastic colored model in a quadrant with domain wall boundary conditions (courtesy of L. Petrov).

$\mathcal{I} = \{I_1 < \dots < I_k\}$  on the top boundary and positions  $\mathcal{J} = \{J_1 < \dots < J_\ell\}$  on the right boundary. We denote this partition function by  $\mathbb{P}_{6v}(\mathcal{I}, \mathcal{J})$ .

The picture on the right is for the partition function in the (stochastic) colored model on a similar rectangle with  $n = N$  colors, no more than one path on each edge, row rapidities  $x_1, \dots, x_N$  numbered *bottom-to-top*, column rapidities  $y_1, \dots, y_M$  (numbered left-to-right), and vertex weights given by (1.5.8) with  $n = N$  and with the spectral parameter  $z$  equal to  $x_i y_j$ , where  $x_i$  and  $y_j$  are the rapidities of the vertex's row and column. The boundary conditions are specified by requiring that a path of color  $i$ ,  $1 \leq i \leq N$ , enters through the horizontal edge in row  $i$  (with rapidity  $x_i$ ) on the left boundary. We also fix the positions (but not the colors) of the paths that exit through the top boundary to be given by  $\mathcal{I}$ , exactly as for the color-blind case, and we fix colors (but not the positions) of the paths that exit through the right boundary to be given by  $\mathcal{J} = \{J_1 < \dots < J_\ell\}$ . We denote this partition function by  $\mathbb{P}_{\text{col}}(\mathcal{I}, \mathcal{J})$ . See Figure 2 for a simulation of the colored model.

**Theorem 1.6.1 (Theorem 10.4.1 below).** — *For any integers  $M, N \geq 1$ , and two integer sets  $\mathcal{I} = \{1 \leq I_1 < \dots < I_k \leq M\}$  and  $\mathcal{J} = \{1 \leq J_1 < \dots < J_\ell \leq N\}$ , the following equality of distributions holds:*

$$(1.6.1) \quad \mathbb{P}_{6v}(\mathcal{I}, \mathcal{J}) = \mathbb{P}_{\text{col}}(\mathcal{I}, \mathcal{J}).$$

This statement also allows for fusion, leading to multiple paths occupying vertical edges; see Theorem 12.2.1.

A weaker version of the Result (1.6.1) was previously obtained in [52]. This earlier result applied to the situation in which  $M = N$ ,  $\mathcal{I} = \{1, \dots, N\}$ , and where the



set  $\mathcal{J}$  is empty, so that all colored paths exit the partition function  $\mathbb{P}_{\text{col}}(\{1, \dots, N\}, \emptyset)$  via its top boundary; see Remark 10.4.2.

The weights (1.5.8) are *stochastic*, which means that the partition function  $\mathbb{P}_{6v}(\mathcal{J}, \mathcal{J})$  can be viewed as the probability, for a Markovian process of propagating paths that entered through the left boundary, to exit the rectangle at prescribed locations. Similarly, the partition function  $\mathbb{P}_{\text{col}}(\mathcal{J}, \mathcal{J})$  is the probability for similarly constructed Markovian *colored* paths to (a) exit through positions  $\mathcal{J}$  on top of the rectangle, and (b) have the set of colors of the paths that exit through the right boundary equal to  $\mathcal{J}$ .

The proof of Theorem 10.4.1 that we give is a non-trivial recursive argument (of the type broadly used in [52, 90]) that may not look particularly illuminating. As a matter of fact, the way we first encountered this matching went through a correspondence with a third partition function related to *colored Hall-Littlewood processes*; let us define it.

Having two positive integers  $M, N \geq 1$ , a composition  $\mu = (\mu_1, \dots, \mu_M)$  of length  $M$ , and a Gelfand-Tsetlin pattern (sequence of interlacing<sup>(3)</sup> partitions)  $\lambda = \{\lambda^{(1)} \succ \dots \succ \lambda^{(N)} = \emptyset\}$  of length  $N - 1$ , associate to this pair of objects the weight

$$(1.6.2) \quad \mathbb{W}_{M,N}(\mu, \lambda) = E_{\tilde{\mu}}(y_M, \dots, y_1) \cdot Q_{\mu^+/\lambda^{(1)}}(x_1) \cdot \prod_{j=2}^N Q_{\lambda^{(j-1)}/\lambda^{(j)}}(x_j) \cdot \prod_{i=1}^N \prod_{j=1}^M \frac{1 - x_i y_j}{1 - q x_i y_j}.$$

Here  $Q$ 's are symmetric (skew) Hall-Littlewood polynomials,  $E$ 's are non-symmetric Hall-Littlewood polynomials,  $\mu^+$  is the nondecreasing ordering of  $\mu$ , and  $(\tilde{\mu}_1, \dots, \tilde{\mu}_M) = (\mu_M, \dots, \mu_1)$ .

For  $0 \leq x_i, y_j < 1$ , this defines a probability measure; the weights (1.6.2) are nonnegative, and they add up to one:

$$(1.6.3) \quad \sum_{\mu} \sum_{\lambda} \mathbb{W}_{M,N}(\mu, \lambda) \equiv 1.$$

This summation follows from the fact that symmetrization of non-symmetric Hall-Littlewood polynomials yields the symmetric ones, and the Cauchy identity for the symmetric Hall-Littlewood polynomials.

Define the *zero set*  $z(\mu)$  of the composition  $(\mu_1, \dots, \mu_M)$  as

$$z(\mu) = \{1 \leq i \leq M : \mu_i = 0\},$$

and a further set

$$\zeta(\mu, \lambda) = \{1 \leq j \leq N : \ell(\lambda^{(j-1)}) - \ell(\lambda^{(j)}) = 0\}, \quad \lambda^{(0)} \equiv \mu^+,$$

which measures the differences between lengths of neighboring partitions in the extended Gelfand-Tsetlin pattern  $\mu^+ \succ \lambda^{(1)} \succ \dots \succ \lambda^{(N-1)} \succ \lambda^{(N)} = \emptyset$ . Further, we

---

3. We write  $\nu \succ \kappa$  or  $\kappa \prec \nu$  if and only if the partitions  $\nu$  and  $\kappa$  interlace, i.e.,  $\nu_1 \geq \kappa_1 \geq \nu_2 \geq \kappa_2 \geq \dots$ .

define (with notation  $\bar{\mathcal{J}} = \{1, \dots, M\} \setminus \mathcal{J}$ )

$$\mathbb{P}_{\text{cHL}}(\mathcal{J}, \bar{\mathcal{J}}) = \sum_{\mu} \sum_{\lambda} \mathbb{W}_{M,N}(\mu, \lambda) \cdot \mathbf{1}_{z(\mu)=\bar{\mathcal{J}}} \cdot \mathbf{1}_{\zeta(\mu,\lambda)=\mathcal{J}},$$

which is the distribution of the random variables  $z(\mu)$ ,  $\zeta(\mu, \lambda)$  in the pair  $(\mu, \lambda)$  sampled with respect to the colored Hall-Littlewood process (1.6.2).

**Theorem 1.6.2 (Theorem 10.5.1 below).** — *For any integers  $M, N \geq 1$ , and two integer sets  $\mathcal{J} = \{1 \leq I_1 < \dots < I_k \leq M\}$  and  $\bar{\mathcal{J}} = \{1 \leq J_1 < \dots < J_\ell \leq N\}$ , the following equality of distributions holds:*

$$(1.6.4) \quad \mathbb{P}_{6v}(\mathcal{J}, \bar{\mathcal{J}}) = \mathbb{P}_{\text{cHL}}(\mathcal{J}, \bar{\mathcal{J}}).$$

Together with Theorem 1.6.1, this also implies

$$(1.6.5) \quad \mathbb{P}_{\text{col}}(\mathcal{J}, \bar{\mathcal{J}}) = \mathbb{P}_{\text{cHL}}(\mathcal{J}, \bar{\mathcal{J}}).$$

We give a proof of (1.6.4) by a graphical argument involving the Yang-Baxter equation. There is also a parallel proof of (1.6.5) that uses graphical arguments and exchange relations similar to (1.5.4), but we leave it out of this paper. Instead, we offer a second proof of (1.6.4) based on different ideas. More exactly, using the results of [61], we compute averages of observables of the colored Hall-Littlewood process by applying Cherednik-Dunkl operators to a version of the Cauchy summation identity (1.6.3), match them to the corresponding observables of  $\mathbb{P}_{6v}(\mathcal{J}, \bar{\mathcal{J}})$  (known thanks to [32, 20]), and prove that the resulting sets of observables are rich enough to identify the measures. We hope that this approach might be extendable to understanding joint distributions of colors of paths passing under multiple locations of the lattice (as opposed to the single vertex  $(M, N)$  in the definition of  $\mathbb{P}_{\text{col}}(\mathcal{J}, \bar{\mathcal{J}})$ ).

## 1.7. Matching for interacting particle systems

The distributional match of Theorems 1.6.1 and 12.2.1 can be followed through various degenerations of the involved stochastic vertex models. In Chapter 12 we give detailed descriptions of how such degenerations work for three continuous time Markov chains—the ASEP, a system of  $q$ -bosons, and an interacting particle system with bounded occupancy of each site that generalizes the system known as the PushTASEP (or long-range TASEP). Let us give a brief description of the ASEP result.

Consider a system of particles on the one-dimensional lattice  $\mathbb{Z}$  with no more than a single particle per site. Assume that the particles have colors that are positive integers (several particles may have the same color, and not all colors need to be utilized). The empty sites, that are also commonly called holes, can be naturally identified with particles of color 0, in which case every site of the lattice is occupied by a particle of a nonnegative color.

The colored ASEP is a continuous time Markov process on the space of such systems of particles. A (somewhat informal) description of the Markovian evolution is as follows: each particle is equipped with a left and a right exponential clock of rates  $q$

and 1, respectively; all the clocks in the system are independent. When the left (resp., right) clock of a particle rings, it checks if the site immediately to the left (resp., right) of its current location is occupied by a particle of a smaller color. If it is, then these two particles are swapped, and if not, then nothing happens.

If all particles of the system are of a single color (not counting the holes), then this evolution reduces to the usual uncolored ASEP. Note that the uncolored ASEP is also the projection of the colored one when the distinctions between the colors (apart from 0) are being ignored. More generally, one can always reduce the number of colors in the colored ASEP by ignoring distinctions between colors in any interval. If particles of only two nonzero colors are present in the system, then the particles of the smaller color behave as *second class particles*, in the conventional ASEP terminology.

We will be concerned with the (*half-*)*Bernoulli* initial condition (at time  $t = 0$ ) defined as follows. Choose  $p \in (0, 1]$ , and for each  $i = 1, 2, \dots$ , place a particle of color  $i$  at location  $(-i)$  with probability  $p$ , independently over all  $i$ . For  $p = 1$  all the sites  $-1, -2, \dots$  are going to be occupied by particles of colors  $1, 2, \dots$ , respectively. We refer to the latter case as the *step* initial condition.

Let us now state the matching result.

Fix an arbitrary integer  $P$  (reference position) and two sets of pairwise distinct integers  $\mathcal{J} = \{I_1 < \dots < I_k \leq P\}$  and  $\mathcal{J}' = \{1 \leq J_1 < \dots < J_\ell\}$ . Consider the following probabilities:

$$\mathbb{P}^{\text{ASEP}}(\mathcal{J}, \mathcal{J}'; P, t) = \text{Prob} \left\{ \begin{array}{l} \text{there is a particle at each of} \\ \text{the locations } I_1, \dots, I_k; P + J_1, \dots, P + J_\ell \end{array} \right\},$$

$$\mathbb{P}^{\text{mASEP}}(\mathcal{J}, \mathcal{J}'; P, t) = \text{Prob} \left\{ \begin{array}{l} \text{there is a particle at each of the locations } I_1, \dots, I_k, \\ \text{and there is a particle of each of the colors } J_1, \dots, J_\ell \\ \text{to the right of location } P \end{array} \right\}.$$

**Theorem 1.7.1 (Theorem 12.3.5 below).** — *Consider the colored ASEP with the half-Bernoulli initial condition, as defined above. Then for all time  $t \geq 0$ , any integer  $P \in \mathbb{Z}$ , and arbitrary integer sets  $\mathcal{J} = \{I_1 < \dots < I_k \leq P\}$  and  $\mathcal{J}' = \{1 \leq J_1 < \dots < J_\ell\}$ , we have*

$$\mathbb{P}^{\text{ASEP}}(\mathcal{J}, \mathcal{J}'; P, t) = \mathbb{P}^{\text{mASEP}}(\mathcal{J}, \mathcal{J}'; P, t).$$

One can show that in the case of step initial condition ( $p = 1$ ) and  $\mathcal{J}' = \emptyset$ , Theorem 1.7.1 also follows from [7, Theorem 1.4]. This does not seem to extend to arbitrary  $p$  and  $\mathcal{J}'$ , however.

Matching results for the colored  $q$ -bosons and the PushTASEP-like colored system that are somewhat similar to Theorem 1.7.1, and that are also derived from the vertex model matching of Theorems 1.6.1 and 12.2.1, are given in Sections 12.4–12.5 below (see Theorems 12.4.2 and 12.5.2, respectively).

## 1.8. Asymptotics

The matching of Theorem 1.6.1 and its extensions gives rise to a host of asymptotic statements for the colored models via the corresponding asymptotics of the color-blind ones. Let us survey the latter ones very quickly.

It is convenient to speak in terms of the *height functions* that count the number of paths/particles to the right (or left) of a given location in the two-dimensional space time. For colored models, one can speak of a *colored* height function that counts the number of paths/particles to the right of a specified location, but only takes into account paths/particles whose color does not exceed a certain cut-off. This turns the height function into a random function of *three* variables rather than two. The matching statements thus provide identities between the distributions of the colored height functions on certain one-dimensional sections of the three-dimensional physical space, and those of the uncolored height functions on one-dimensional sections of the two-dimensional physical space.

The large time/space/color asymptotics for the models considered in the present work can be of (at least) four different types; in terms of the color-blind models, they correspond to:

1. A local limit regime with observed space locations at finite distance from each other and the limiting object typically being a product of Bernoulli measures or their generalization (local equilibrium).
2. Global Gaussian random field asymptotics with observation points ranging over the whole active region of the physical space, in the case of symmetric models ( $q = 1$ ), or weakly asymmetric ones ( $q \rightarrow 1$ ) with relatively small, but still diverging scaling of space/time.
3. In the weakly asymmetric case, intermediate space/time scaling and appropriate mesoscopic distances between observation points yield limiting random polymers in random media, *e.g.*, the KPZ equation.
4. In the asymmetric case ( $q \neq 1$  is fixed), or the weakly asymmetric case at large scales, mesoscopic distances between observation points produce a broadly universal limiting object known as the *KPZ fixed point*.

Note that in order to use the matching for deriving a non-trivial colored result from an uncolored one, one needs to know *process level* convergence of the uncolored height function as the one-point distributions match trivially. This substantially reduces the number of rigorously known results; there are, however, widely believed conjectures and heuristic arguments wherever the one-point convergence is known.

For (1), the very first result is the behavior of the particle of color 1 in the colored TASEP, and our matching result says that it is asymptotically equivalent to the color-blind TASEP density. This is a celebrated result of Ferrari-Kipnis [51] about the second class particle in a rarefaction fan. Its extensions to many colors for the ASEP with step initial condition have been investigated by Amir-Angel-Valko [7] via a matching result that is not far from (the ASEP degeneration of) ours. For a single

second class particle, a recent work by Balázs-Nagy [11] proves results for more general (continuous time) processes, again by a suitable matching.

For (2), the asymptotic behavior of the uncolored height function is a deterministic law of large numbers (hydrodynamic limit) given by a first order PDE, and Gaussian fluctuations around it are given by a solution of a stochastic PDE that is a classical second order PDE with a white noise inhomogeneity, cf. De Masi-Presutti-Scacciatelli [45], Dittrich-Gärtner [47], Borodin-Gorin [29], Shen-Tsai [81] and references therein. No colored results or conjectures have been previously known.

For (3), the uncolored height function converges to the logarithm of the partition function for a finite temperature directed polymer in a Gaussian random medium, see, Bertini-Giacomin [15] and [8] for the ASEP and the continuum polymer (equivalently, the KPZ equation), Borodin-Corwin [21] for the  $q$ -TASEP and the O’Connell-Yor (semi-discrete) polymer, Corwin-Tsai [44] and Corwin-Ghosal-Shen-Tsai [42] for the stochastic six vertex and the continuum polymer. No colored results or conjectures have been previously known.

For (4), only for the TASEP and PushTASEP (as well as for a few closely related, *determinantal* models) process level convergence results have been rigorously established, cf. Borodin-Ferrari [27], Matetski-Quastel-Remenik [75]; conjectures, however, are broadly available, cf. Corwin [40], Spohn [82], Corwin-Dimitrov [41]. No colored results have been previously known. The only available colored predictions have been made by Spohn [83], but it remains unclear whether they are applicable to any of the models covered by our matchings.

It would be extremely interesting to access any of the outlined asymptotic results without employing the matching, but rather through utilizing the spectral analysis of the transfer-matrices described above. We leave this to a future work.

## 1.9. A word about extensions

The algebraic formalism of the present work should be readily extendable to:

- Inhomogeneous lattice models, similarly to what was done in [32] in the color-blind case;
- The spin  $q$ -Whittaker functions, similarly to what was done in [33] in the color-blind case;
- Elliptic and trigonometric IRF (Interaction-Round-a-Face) or SOS (Solid-On-Solid) models, similarly to what was done in [19], [2] in the color-blind case.

We chose to leave these more general scenarios out of the scope of this paper that, as it is, ended up pretty long.

## 1.10. Acknowledgments

A. B. was partially supported by the NSF grant DMS-1607901 and DMS-1664619. M. W. was partially supported by the ARC grant DE160100958.